UNCOUPLED DYNAMIC FRACTURE APPROACH

J.C.W. van Vroonhoven[1]

An uncoupled approach for the analysis of dynamic crack propagation is proposed. This new approach consists of two steps. Firstly, the elastodynamic stresses are calculated for the undamaged elastic body. In this calculation it is assumed that there are no cracks. Secondly, possible crack patterns are derived from the stress data with the use of stress-intensity factors for slightly curved cracks and a dynamic fracture criterion. The advantages of the uncoupled approach are its ease-of-use and the little computational effort.

INTRODUCTION

Problems of dynamic fracture involve stress waves and crack propagation. There exists a certain interaction between these effects: the (dynamic) stresses determine the crack propagation, while rapid fracture initiates new stress waves. This interaction can be incorporated in a full-scale dynamic fracture analysis. The advantage of such analysis is that fracture-mechanics methods have been studied extensively and possess a high degree of accuracy. A strong disadvantage, however, occurs when the finite-element method is applied to problems of dynamic crack propagation. Because of the material rupture and the creation of new crack surfaces, the geometry of the elastic body changes continuously. This necessitates a continuous adaptation of the element mesh, a shift of the singular crack-tip elements to the new position of the crack tip, and an interpolation of the mechanical quantities from the old to the new element division. These moving-element techniques require much computing time, because the assembly of all element contributions into one global stiffness matrix must be repeated after each crack increment. Therefore, an alternative approach towards dynamic failure analysis is proposed.

[1]Philips Research Laboratories, Prof. Holstlaan 4, 5656 AA Eindhoven, The Netherlands.

The uncoupled dynamic fracture approach [1] is based on the elastodynamic stresses calculated for the undamaged configuration. The dynamic response of the elastic body to a time-dependent load is determined first. Afterwards, as a form of post-processing, predictions of crack patterns are derived from the dynamic stress data. The interaction between the crack propagation and the stress waves is only partially accounted for in this uncoupled analysis, because the disturbing effect of crack propagation on the stress distribution is neglected. Also, the mutual influence of multiple cracks is not incorporated. Of course, it cannot be expected that this uncoupled approach will produce highly accurate results for the entire fracture process, especially near the moment of final collapse. Nevertheless, it is possible to analyse the initial stages of crack propagation with reasonable accuracy and with limited numerical effort.

DESCRIPTION OF THE METHOD

The first step in the uncoupled approach is the calculation of the dynamic stresses in the elastic body as function of time, e.g. by the finite-element method. It is assumed that the material remains linearly elastic and that no cracks are present.

The second step is the initiation of a crack. We assume the existence of a crack at a certain position and at a given moment of time. The location, length, and direction of this crack can be chosen freely. The crack, however, is a virtual crack in the sense that it does not exist in reality. The stresses in the positions where the crack is assumed, are considered to act on the crack surfaces, opening the crack, and creating a stress intensity at its tip.

The third step in the uncoupled fracture approach is the determination of the crack path. After the initiation of the crack and at any intermediate stage of the fracture calculation, we must calculate both the speed and the direction of further crack propagation. Concerning the dimensions of the elastic body, we restrict ourselves to thin-walled, plate-like structures with slight curvature such that we may use the approximation of a thin, flat plate containing a through-thickness crack. As a result, we may employ the well-known expressions for the stress-intensity factors for cracks in plates [2, 3, 4]. The thickness of the plate is denoted by h and the shape of the curved crack is represented by the function $y = \lambda(x)$ for $-a \leq x \leq +a$. This crack-shape function is determined by measurement of the distance to the line connecting the end points of the crack path, as shown in Fig. 1. So, we have $\lambda(\pm a) = 0$. The directions normal and tangential to the crack surfaces are denoted by n and s, while the z-direction is perpendicular to the plate.

The stresses along the crack are derived from the elastodynamic stresses calculated at step one and are denoted by $\sigma_{ij}(x,t)$ at time t. The stress-intensity factors K_I and K_{II} for a curved crack loaded by in-plane tensile and shear forces $\sigma_{nn}(x,t)$ and $\sigma_{ns}(x,t)$ are determined with the use of the results of

Cotterell and Rice [2]. The factor K_{III} for a curved crack loaded by transverse shear forces $\sigma_{nz}(x,t)$ has been calculated in [4]. The stress-intensity factors k_1 and k_2 for a curved crack loaded by out-of-plane bending and twisting moments $M_{nn}(x,t)$ and $M_{ns}(x,t)$ have been calculated in [3] on the basis of classical plate theory. These factors are expressed in terms of the function $\lambda(x)$ and the respective stresses and moments.

The fracture criterion is based on the J-integrals. The relations with the stress-intensity factors are given by (see [1, 3] and Hui and Zehnder [5])

$$J_1 = \frac{h}{E}\left(K_I^2 + K_{II}^2\right) + \frac{h}{3E}\left(k_1^2 + k_2^2\right) + \frac{h}{2G} K_{III}^2 , \tag{1}$$

$$J_2 = -\frac{2h}{E} K_I K_{II} - \frac{2h}{3E} k_1 k_2 , \tag{2}$$

where E and G are the Young's and shear moduli of the material.

The direction of crack propagation is derived from the direction of the J-integral vector. The crack-propagation angle θ_P is measured with respect to the tangent to the crack surface, at the crack tip. According to Cherepanov [6, Ch. 5] we have

$$\tan \theta_P = \frac{J_2}{J_1} . \tag{3}$$

The speed of crack propagation is derived with the use of a dynamic fracture criterion. According to Freund [7, Sec. 6.4] the energy release rate for a dynamic problem equals the energy release rate for the corresponding static equilibrium problem multiplied by a universal function of crack speed. The length of the J-integral vector is then interpreted as the equilibrium energy release rate and the crack-propagation speed c is determined by

$$g(c)\sqrt{J_1^2 + J_2^2} = \mathcal{G}_C , \tag{4}$$

where $\mathcal{G}_C$ is the critical energy release rate. A good approximation for the universal function of crack speed $g(c)$ is

$$g(c) = (1 - c/c_R)\sqrt{1 - c/c_D} , \tag{5}$$

where c_R and c_D are the speeds of Rayleigh waves and dilatational waves.

The new position $\mathbf{x} = (x, y)$ of the crack tip is now calculated as

$$\mathbf{x}_{tip,new} = \mathbf{x}_{tip,old} + \mathbf{c} \cdot \Delta t_{CR} , \tag{6}$$

where $\mathbf{c}$ is a vector with length c and with its direction determined by the angle θ_P. The time step Δt_{CR} for the crack increment may be larger than the time step Δt_{FE} used for the finite-element computation of the elastodynamic stresses, because the crack speed is always much less than the stress-wave speed. The time step Δt_{CR} should not be chosen too large, because otherwise the condition for stability of the algorithm (6) will be violated.

EXAMPLES

The uncoupled fracture approach has been applied to a single-edge notched beam of length 440 mm, height 100 mm, and thickness 10 mm (see [1] and Fig. 2). Forces F_1 and $F_2 = F_1/10$ are applied such that a shear-stress situation arises in the middle section of the beam. A crack with length 15 mm is initiated at the middle of the bottom edge of the beam. Crack propagation occurs along a curved path and must end at the upper edge of the beam to the right of the point where the force F_1 is applied [8]. The crack pattern of Fig. 2 agrees with both the experimental and the numerical results of Schlangen [8], although deviations occur near the point of crack arrest.

As a three-dimensional example we have studied a hollow cylindrical pipe of length 400 mm and inner and outer radii 30 and 40 mm, which is loaded by torsional moments at both end surfaces (see [1] and Fig. 3). A through crack is initiated in the middle cross section of the pipe. Crack propagation has been calculated in two (symmetric) directions. The results are shown in Figs. 3–4 and agree with the experimental work of Richard [9].

CONCLUSIONS

An effective and low-cost method for fracture calculations has been established. The great benefit of this uncoupled fracture approach is that a continuous adaptation of the finite-element division is not necessary. In addition, the stresses calculated by one elastodynamic finite-element analysis can be used repeatedly for multiple crack computations. The method has been applied to various problems in two and three dimensions. Reliable crack-path predictions have been obtained for the early stages of (mixed-mode) fracture with rather limited computational effort.

REFERENCES

1. J.C.W. van Vroonhoven, *Dynamic Crack Propagation in Brittle Materials: Analyses Based on Fracture and Damage Mechanics.* PhD Thesis, Eindhoven University of Technology, The Netherlands (1996).
2. B. Cotterell and J.R. Rice, *Int. J. Fracture* 16 (1980) 155–169.
3. J.C.W. van Vroonhoven, *Int. J. Fracture* 68 (1994) 193–218.
4. J.C.W. van Vroonhoven, *Int. J. Fracture* 70 (1995) 1–18.
5. C.Y. Hui and A.T. Zehnder, *Int. J. Fracture* 61 (1993) 211–229.
6. G.P. Cherepanov, *Mechanics of Brittle Fracture.* McGraw–Hill (1979).
7. L.B.Freund, *Dynamic Fracture Mechanics.* Cambridge Univ.Press (1990).
8. E. Schlangen, *Experimental and Numerical Analysis of Fracture Processes in Concrete.* PhD Thesis, Delft University of Technology (1993).
9. H.A. Richard, *In: Structural Failure, Product Reliability and Technical Insurance,* H.P. Rossmanith (Ed.), Inderscience, Geneva (1987) 423–437.

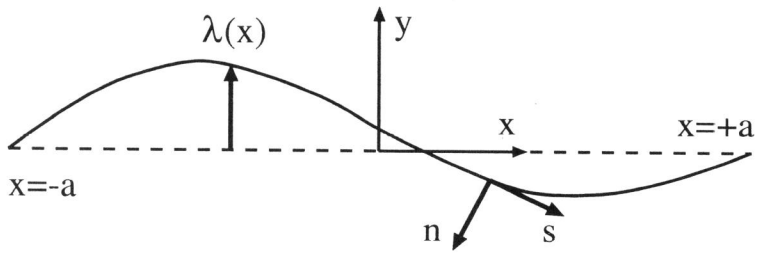

Figure 1: Geometry of curved crack.

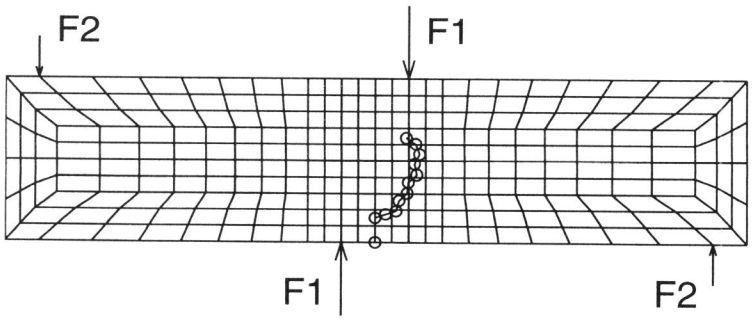

Figure 2: Crack pattern in single-edge notched beam loaded under shear conditions. Crack is initiated at bottom edge of beam.

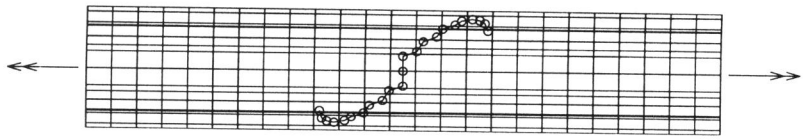

Figure 3: Crack pattern in hollow cylindrical pipe loaded by torsional moments. (a) Side view.

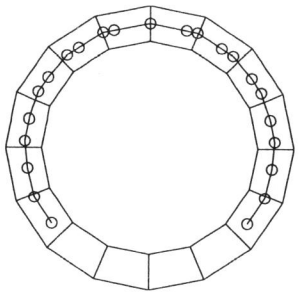

Figure 4: Crack pattern in hollow cylindrical pipe loaded by torsional moments. (b) Cross-sectional view.